npg

ORIGINAL ARTICLE

BAG-1 overexpression attenuates luminal apoptosis in MCF-10A mammary epithelial cells through enhanced RAF-1 activation

LR Anderson[1], RL Sutherland[1,2] and AJ Butt[1,2]

[1]Cancer Research Program, Garvan Institute of Medical Research, Darlinghurst, Sydney, New South Wales, Australia and
[2]St Vincent's Clinical School, Faculty of Medicine, University of New South Wales, Sydney, New South Wales, Australia

Although the multi-functional, prosurvival protein, Bcl-2-associated anthanogene 1 (BAG-1) is frequently over-expressed in breast cancers, its role in the development or maintenance of the malignant state remains unclear. Here, we have used the established MCF-10A 3-dimensional (3D) model of mammary morphogenesis as a biologically relevant system to determine how BAG-1 expression may influence the development of breast cancer. When cultured in 3D, MCF-10A cells undergo a highly regulated morphogenic program leading to the development of polarized acinar structures containing a central, hollow lumen formed, in part, through the induction of BIM-dependent apoptosis. BAG-1 over-expression resulted in an attenuation of this normal apoptotic program characterized by a significantly increased number of acini with filled lumens—a phenotype commonly observed in ductal carcinoma *in situ*. BAG-1's effects were associated with an activation of RAF-1—a known binding partner of BAG-1, enhanced signaling through the MAP kinase pathway and a decrease in BIM expression. Reversal of the BAG-1-associated survival phenotype by the mitogen-activated kinase/ERK kinase inhibitor, U0126, implicates the RAF-1–extracellular signal-regulated kinase signaling pathway as a major mediator of BAG-1's effects in this model. As BAG-1 expression is often elevated in preinvasive breast cancers, these findings support a possible role for BAG-1 as an early contributor to the malignant process in the breast.
Oncogene (2010) 29, 527–538; doi:10.1038/onc.2009.362; published online 2 November 2009

Keywords: BAG-1; breast cancer; apoptosis; RAF-1; ERK; MCF-10A

Introduction

BAG-1 (BCL-2-associated anthanogene 1) is a prosurvival protein that was first identified as a binding partner of BCL-2 (Takayama *et al.*, 1995) and the activated glucocorticoid receptor (Zeiner and Gehring, 1995), and has subsequently been shown to have pleiotropic effects on a diverse range of cellular responses, including apoptosis, transcription, proliferation and signaling (Townsend *et al.*, 2003b).

The *BAG-1* gene encodes three major protein isoforms: designated BAG-1S (36 kDa), BAG-1M (46 kDa) and BAG-1L (50 kDa), which are generated by alternate translation initiation from a single mRNA molecule and share a common carboxy terminus (Townsend *et al.*, 2003b). The latter contains the 'BAG domain', a region that has a key role in mediating many of BAG-1's cellular effects. Interaction between BAG-1 and the heat shock proteins, HSC70 and HSP70, is mediated through the BAG domain and it regulates the refolding of denatured substrate proteins into functional conformations, particularly in response to cellular stress (Höhfeld, 1998). It is also the region mediating interactions between BAG-1 and the serine/threonine protein kinase, RAF-1 (Wang *et al.*, 1996; Song *et al.*, 2001), with evidence of competition between RAF-1 and HSP70 for BAG-1 binding (Song *et al.*, 2001). Ras-induced activation of RAF-1 transmits proliferative and prosurvival signals from extracellular, mitogenic growth factors leading to the activation of mitogen-activated kinase/ERK kinase (MEK) and extracellular signal-regulated kinase (ERK; for review, see Kolch (2000)). However, BAG-1's activation of RAF-1 is independent of Ras signaling and is negatively regulated by HSP70 (Song *et al.*, 2001), thus possibly defining a new link between the cellular stress response and the regulation of cell growth and survival.

The unique amino terminus of BAG-1 mediates the intracellular localization of the isoforms with BAG-1L containing a nuclear localization signal consistent with its predominantly nuclear expression, and BAG-1S and BAG-1M (both lacking the nuclear localization signal) located in the cytoplasm and cytoplasm/nucleus, respectively (Packham *et al.*, 1997; Takayama *et al.*, 1998). This differential localization may also dictate functional differences between the isoforms. For example, only BAG-1L interacts with the nuclear hormone receptors, estrogen receptor (ER) and androgen receptor leading to an enhancement in their transcriptional activity (Froesch *et al.*, 1998; Cutress *et al.*, 2003).

One of the most commonly studied of BAG-1's cellular functions is its effect on cellular survival, although the underlying molecular mechanisms involved

are yet to be fully elucidated. BAG-1 is induced by a variety of survival signals and suppresses apoptosis initiated by a diverse range of stimuli, including chemotherapeutic agents such as etoposide and cisplatin, radiation, death receptor activation and growth factor withdrawal (for review, see Townsend *et al.* (2003b)).

There are a number of possible mechanisms by which BAG-1 may mediate its pro-survival effects. It is known to interact with and enhance the activity of the anti-apoptotic regulator, BCL-2 (Takayama *et al.*, 1995), with evidence of their colocalization at the mitochondria (Takayama *et al.*, 1998)—the key organelle involved in regulating the intrinsic apoptotic pathway. It has also been suggested that BAG-1–HSP70 complexes may enhance the activity of BCL-2 by effecting a conformational change in the latter (Takayama *et al.*, 1997), although direct evidence for this is lacking. Certainly, BAG-1's interactions with the molecular chaperones, HSP70 and HSC70, seem to be important for its prosurvival function as mutation of the heat shock-protein-binding site in BAG-1S abrogates its ability to protect against heat shock-induced apoptosis (Townsend *et al.*, 2003a). Furthermore, as BAG-1's interaction with RAF-1 was maintained in these experiments, it would suggest that BAG-1-induced RAF-1 activation is not critical for anti-apoptotic signaling, at least in this context. However, this may well be a cell type- and stimulus-specific effect, as RAF-1 is known to elicit prosurvival signals through ERK-mediated phosphorylation of pro- and anti-apoptotic effectors such as BAD, BIM and BCL-2 (Kolch, 2000). Recently, Wang *et al.* demonstrated BAG-1's ability to interact with and inhibit the transactivating function of p73, suggesting that this may contribute to BAG-1-mediated survival given p73's known role as a regulator of stress-induced apoptosis (Wang *et al.*, 2009). Thus, BAG-1's pro-survival effects are likely to be mediated through multiple pathways depending on the cellular context and reflecting its numerous and varied binding partners.

The dysregulation of apoptotic signaling pathways is a hallmark of breast cancer like many other malignancies (Hanahan and Weinberg, 2000), and several clinical studies by us and others have attempted to delineate the role of BAG-1 as a potential prognostic or predictive marker in this context. One consistent finding from both *in vitro* and clinical studies is that BAG-1 expression is elevated in breast cancer compared with normal breast epithelium (Takayama *et al.*, 1998; Yang *et al.*, 1999; Turner *et al.*, 2001; Millar *et al.*, 2008). Furthermore, overexpression of the BAG-1S and BAG-1L isoforms in the ER-positive breast cancer cell line, ZR-75-1, significantly enhanced tumor growth in murine xenograft studies compared with control-transfected cells (Kudoh *et al.*, 2002). Interestingly, BAG-1 expression is also elevated in preinvasive breast cancers such as ductal carcinoma *in situ*, as well as precancerous breast lesions (Brimmell *et al.*, 1999), suggesting it may have a role at an early stage in the malignant process. However, the exact nature of BAG-1's effects on the development of breast cancer and the mechanistic basis for its actions in this context remain ill defined. In an attempt to address this, we have used an established three-dimensional (3D) model of mammary epithelial morphogenesis in the immortalized mammary epithelial cell line, MCF-10A (Debnath and Brugge, 2005), to determine how BAG-1 expression might influence key processes leading to breast cancer development in a biologically relevant context. Here we show that BAG-1 expression significantly attenuates the normal apoptotic program in 3D acinar structures, with evidence that this is driven by enhanced activation of RAF-1 signaling and decreased expression of the pro-apoptotic effector, BIM.

Results

Elevated BAG-1 *mRNA and protein expression in breast cancer cell lines compared with normal and immortalized mammary epithelial cells*
BAG-1 mRNA and protein expressions were examined in a panel of cancer (both ER-positive and ER-negative), normal and immortalized breast cell lines by quantitative real-time PCR and immunoblot, respectively. All three of the major BAG-1 protein isoforms (BAG-1L, BAG-1M and BAG-1S) were detected at varying degrees in all of cell lines examined. Figures 1a and b demonstrate that there was a significant increase in *BAG-1* mRNA and protein expression in breast cancer cell lines compared with normal and immortalized breast cells, and supports data from previous studies (Brimmell *et al.*, 1999; Yang *et al.*, 1999). However, no significant differences in BAG-1 expression were observed between ER-positive and ER-negative breast cancer cell lines (data not shown). Interestingly, we did observe differences between mRNA and protein expression levels in the different cell lines, for example, MDA-MB-468 cells have relatively high levels of mRNA but relatively low levels of BAG-1 protein. These results support data from studies on primary breast cancers (Townsend *et al.*, 2002), and suggest that posttranslational control mechanisms are important in dictating BAG-1 expression.

To determine the effects of BAG-1 expression on the malignant process in the breast, BAG-1 was expressed in the immortalized human mammary epithelial cell line, MCF-10A, by retroviral infection. Figure 1c demonstrates that all three major BAG-1 protein isoforms were expressed in MCF-10A/BAG-1 cells at levels comparable with or higher than those observed in breast cancer cell lines.

BAG-1 expression attenuates luminal apoptosis in 3D cultures
When cultured on reconstituted basement membrane (Matrigel; BD Biosciences, San Jose, CA, USA), MCF-10A cells undergo a well-defined morphogenic program leading to the development of polarized acinar structures with a hollow lumen, resembling the mammary lobules in the human breast. The lumen is formed by apoptosis driven by the pro-apoptotic BH3-only protein, BIM and characterized by the expression of active caspase-3 (Debnath and Brugge, 2005).
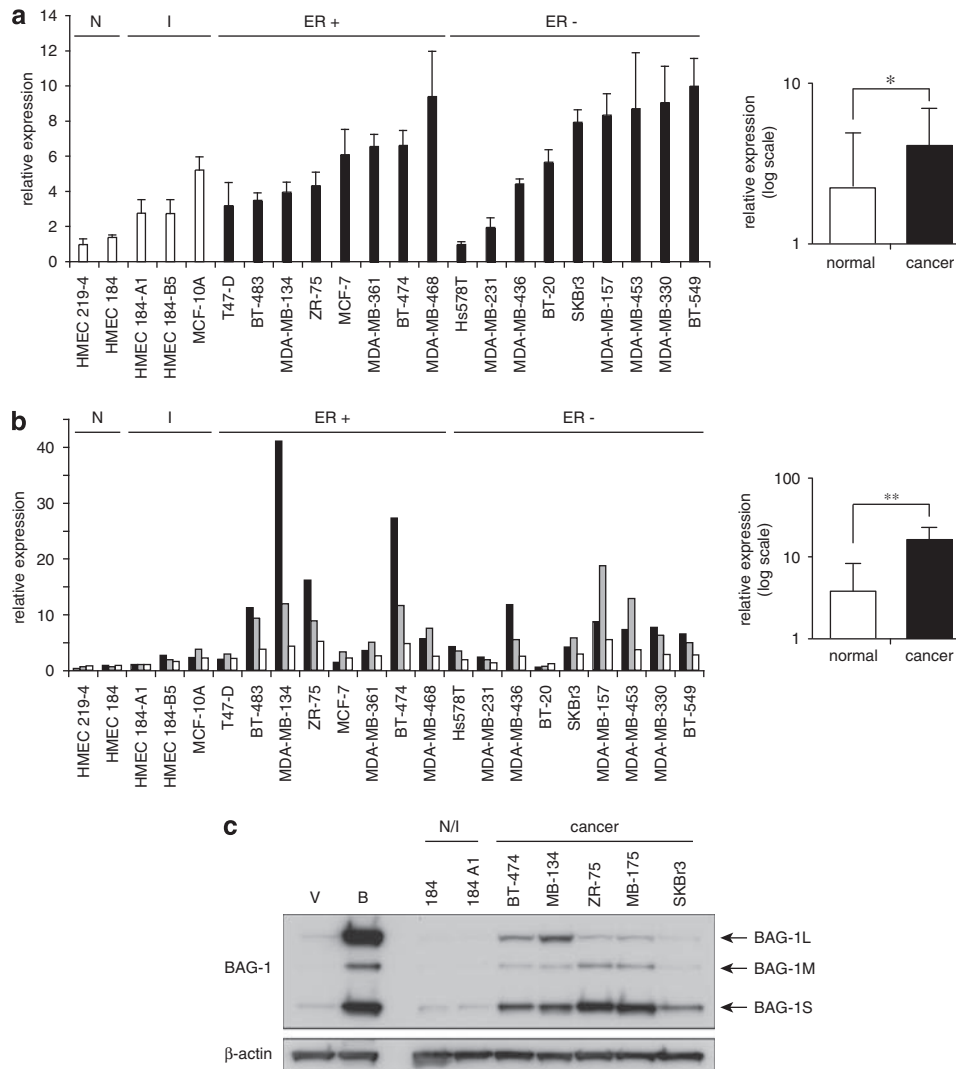
Figure 1 Bcl-2-associated anthanogene 1 (*BAG-1*) mRNA and protein expression levels are elevated in human breast cancer cell lines compared with normal and immortalized breast cell lines. (**a**) *BAG-1* mRNA expression in a panel of ER-positive and ER-negative breast cancer cell lines (black bars) and normal and immortalized breast epithelial cells (white bars), normalized to ribosomal phosphoprotein PO (RPLPO) loading control. Bars represent means of triplicate samples. Representative data from two independent experiments are shown. Graph represents overall levels of *BAG-1* mRNA in normal/immortalized versus cancer cell lines following Log10 transformation. (**b**) Densitometric analysis of BAG-1 protein expression in breast cancer cell lines and normal and immortalized breast epithelial cells. Levels of BAG-1S (black bars), BAG-1M (grey bars) and BAG-1L (white bars) are indicated, normalized to β-actin loading control. Representative data from two independent experiments are shown. Graph represents combined levels of all isoforms in normal/immortalized versus cancer cell lines following Log10 transformation. Error bars indicate 95% confidence intervals, *P<0.05; **P<0.02 for cancer cell lines versus normal/immortalized cells. (**c**), BAG-1 protein expression in MCF-10A stably overexpressing BAG-1 (**b**) and vector controls (*V*), two normal breast epithelial and six breast cancer cell lines. β-actin was used as a loading control.

We examined the effects of BAG-1 expression on luminal apoptosis in 3D acini using both morphological and biochemical markers of this process. First, we determined the amount of luminal clearing in BAG-1-expressing and vector control acini at day 20 of 3D culture when completely hollow lumens are normally present (Mailleux *et al.*, 2008). Figure 2a shows representative confocal images of partial lumen formation in MCF-10A/BAG-1 acini compared with complete lumen formation in MCF-10A/VEC acini. The quantification of lumen formation revealed a significant increase in acini showing no luminal clearing and

significant decrease in partial or fully-cleared lumen in BAG-1-expressing acini compared with vector controls (Figure 2a).

Luminal apoptosis was also detected and quantified by immunostaining with an antibody against M30, a molecular marker of apoptosis that detects caspase-cleaved cytokeratin 18. Under normal conditions, cells in the central luminal space undergo apoptosis between days 7 and 10 of 3D culture (Debnath and Brugge, 2005). BAG-1-expressing acini displayed significantly reduced levels of M30 staining (defined as containing four or more M30-positive cells) at days 7 and 10 of 3D
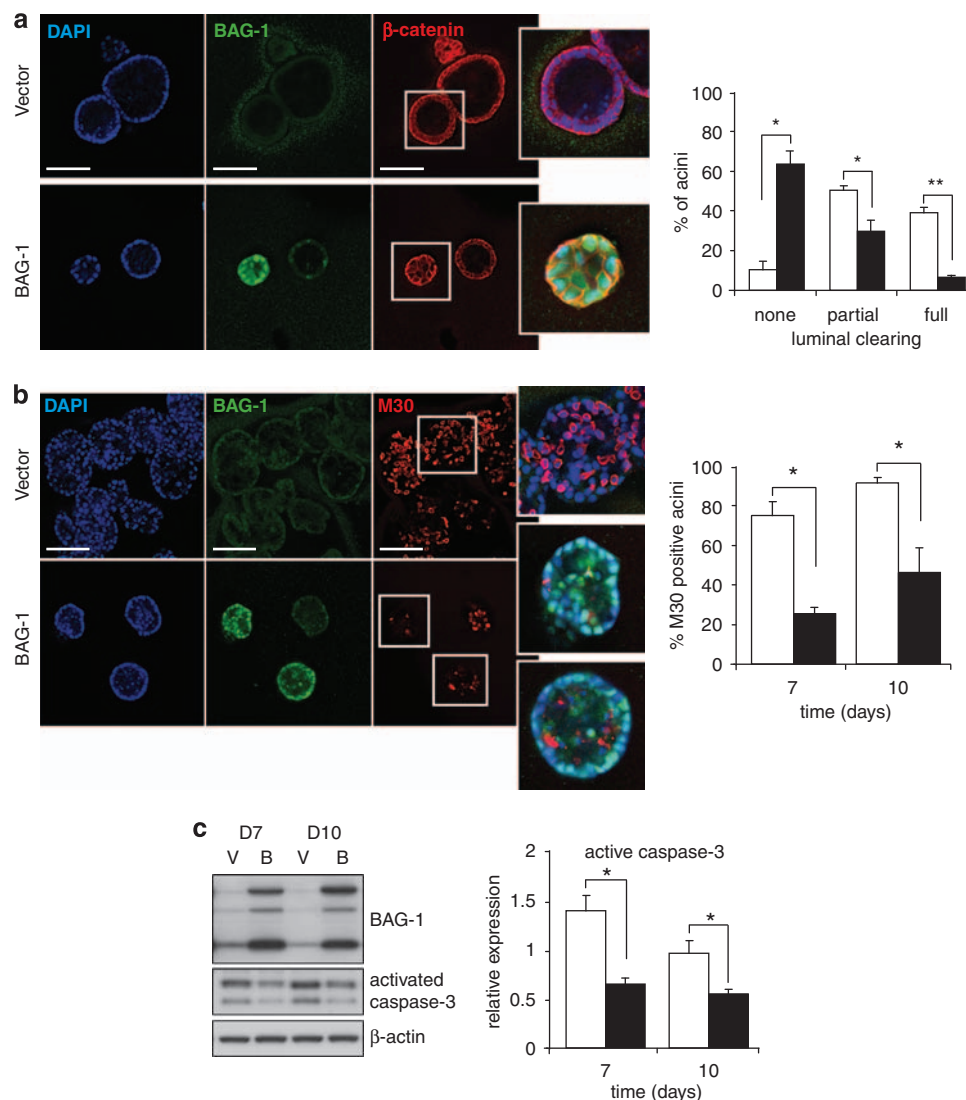
Figure 2 Bcl-2-associated anthanogene 1 (BAG-1) overexpression attenuates luminal apoptosis in three-dimensional (3D) acini. (**a**) Representative equatorial confocal cross-sections showing β-catenin (cell–cell junctions), BAG-1 and 4′,6-diamidino-2-phenylindole (DAPI) (nucleus) staining in BAG-1-overexpressing and vector control acini at day 20 of 3D culture. Overlays of selected sections are shown in the white boxes. Graph represents quantification of luminal clearing in MCF-10A/BAG-1 (black bars) and MCF-10A/VEC acini (white bars) from at least three independent experiments. (**b**) Representative equatorial confocal cross-sections showing M30 (apoptosis), BAG-1 and DAPI staining in BAG-1-expressing and vector control acini at day 10 of 3-D culture. Overlays of selected sections are shown in the white boxes. Scale bars = 100 μm. Graph represents quantification of positive M30 staining (containing ⩾4 M30-positive cells) in MCF-10A/BAG-1 (black bars) and MCF-10A/VEC (white bars) acini at days 7 and 10 from at least three independent experiments. (**c**) Representative immunoblots of activated caspase-3 and BAG-1 expression in lysates from MCF-10A/ BAG-1 (**b**) and MCF-10A/VEC (*V*) acini at day 7 and 10. β-actin was used as a loading control. Graph shows densitometry of cleaved caspase-3 expression normalized to β-actin in MCF-10A/BAG-1 (black bars) and MCF-10A/VEC (white bars) acini from at least three independent experiments. Error bars indicate s.e.m., *$P < 0.05$; **$P < 0.005$ for BAG-1-expressing acini versus vector controls.

culture compared with vector control acini (Figure 2b). In addition, immunoblot of whole-cell lysates from MCF-10A/VEC and BAG-1-expressing acini showed that BAG-1 expression was associated with significantly decreased levels of activated caspase-3 at these same time points compared with vector controls (Figure 2c).

BAG-1-mediated attenuation of luminal apoptosis is associated with increased RAF-1 activation
BAG-1 binds to and activates the serine/threonine protein kinase, RAF-1 *in vitro* (Wang *et al.*, 1996; Song

et al., 2001), which itself can enhance cellular survival signals through ERK-mediated phosphorylation and inactivation of BIM (Kolch, 2000). Thus, to explore a possible mechanistic basis for BAG-1's effects on MCF-10A survival, we examined the phosphorylation of RAF-1 by immunoblotting of cell lysates from MCF-10A/VEC and MCF-10A/BAG-1 acini at days 7 and 10 of 3D culture. Although activation of RAF-1 occurs by phosphorylation at multiple activating sites, serine 338 (S338) is one of the first sites to be phosphorylated (Avruch *et al.*, 1994). A significant increase in RAF-1 S338 phosphorylation was observed

in BAG-1-expressing acini at both time points compared with vector control acini (Figure 3a and b). We then determined whether this was associated with a direct interaction between RAF-1 and BAG-1. Co-immuno-precipitation studies were not readily feasible in 3D culture because of the large numbers of cells required for optimal results. However, RAF-1 and BAG-1 were specifically co-immunoprecipitated from MCF-10A/

BAG-1 cells grown in monolayer culture (Figure 3c) under conditions that mimic the 3-D environment, in which epidermal growth factor is essential for acinar morphogenesis (Brummer et al., 2006). We also examined the intracellular expression of BAG-1 and RAF-1 in MCF-10A by immunocytochemistry and observed a colocalization between the two proteins in MCF-10A/BAG-1 cells (Figure 3d), providing further evidence
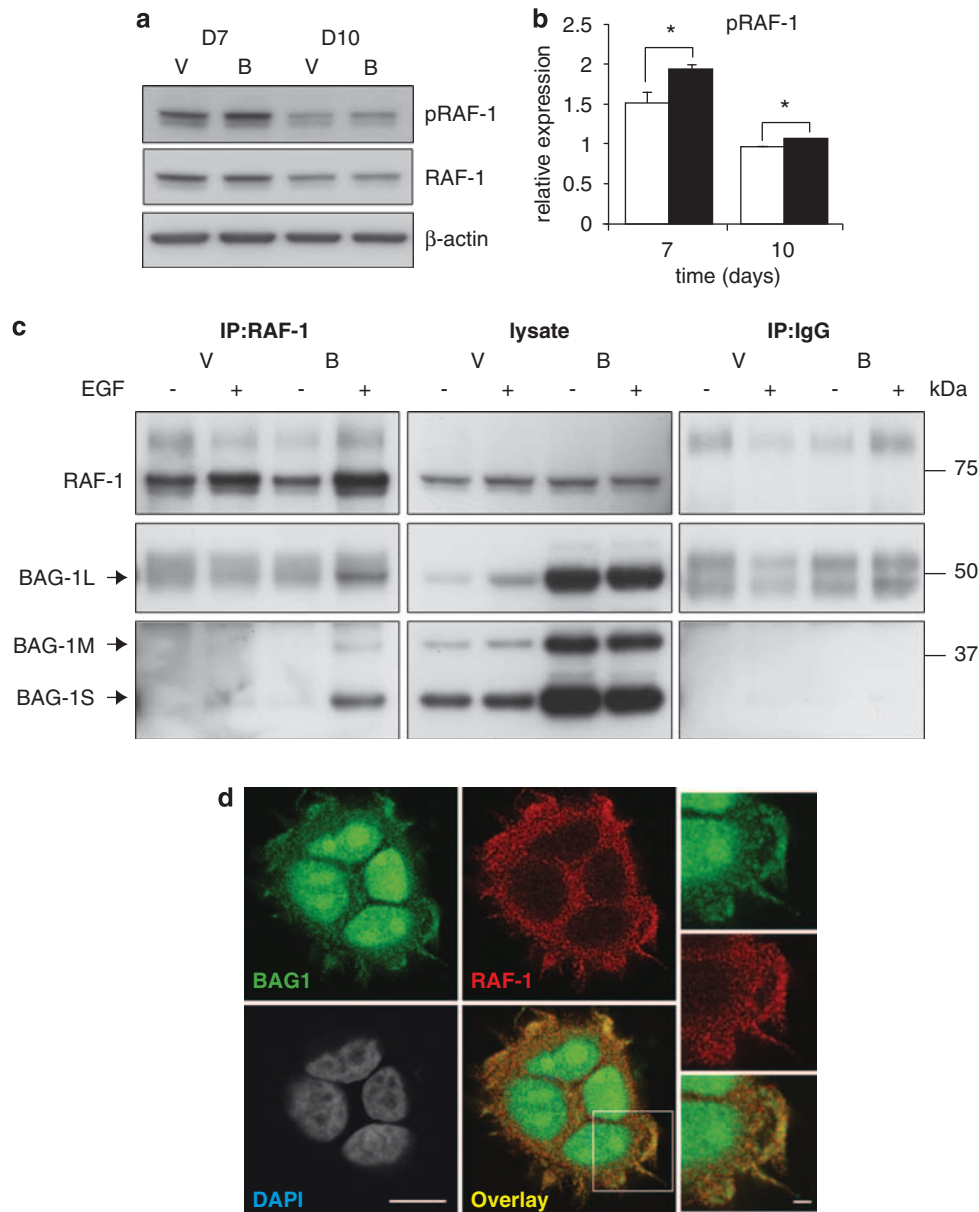

Figure 3 Enhanced RAF-1 activation in Bcl-2-associated anthanogene 1 (BAG-1)-expressing acini. (a), Representative immunoblots of total and serine 338 (S338)-phosphorylated RAF-1 expression in whole-cell lysates from BAG-1-expressing (b) and vector control (V) acini at days 7 and 10 of three-dimensional (3D) culture. β-actin was used as an additional loading control. (b) Densitometry of RAF-1 S338 phosphorylation relative to total RAF-1 at days 7 and 10 in MCF-10A/BAG-1 (black bars) and MCF-10A/VEC (white bars) acini from at least three independent experiments. Error bars indicate s.e.m., *$P < 0.05$ for BAG-1-expressing acini versus vector controls. (c) Immunoprecipitations of lysates from MCF-10A/VEC and MCF-10A/BAG-1 cells were performed using anti-RAF-1 antibody or IgG control where indicated and analysed for RAF-1 or BAG-1 expression. (d) Representative equatorial confocal cross-sections showing BAG-1 and RAF-1 staining in BAG-1-expressing MCF-10A cells. Each image represents an average projection of four z sections. Scale bar = 10 μm. Magnified selected section shown in the white box represents a single confocal slice of a region of BAG-1–RAF-1 colocalization. Scale bar = 2 μm.

supporting a direct interaction. Scoring of approximately 200 cells from two independent experiments for overlap in BAG-1 and RAF-1 expression demonstrated a colocalization of the two proteins in 52.8% (± 2.5 s.e.) of cells.

BAG-1-mediated survival is associated with increased ERK1/2 phosphorylation and decreased BIM expression

To further explore the role of RAF-1 activation in mediating BAG-1's pro-survival effects, we examined downstream components of the MEK–ERK signaling cascade, namely increased phosphorylation of ERK1/2 and decreased expression of BIM_{EL} (Kolch, 2000). Figures 4a and b demonstrate that BAG-1 expression was associated with a significant increase in ERK1/2 phosphorylation at days 7 and 10 of 3D culture when compared with vector control acini. In addition, a significant decrease in BIM_{EL} expression was observed at these time points in MCF-10A/BAG-1 acini compared with MCF-10A/VEC acini (Figures 4a and c). These data suggest that BAG-1 expression is associated with enhanced signaling through the MEK–ERK signaling pathway downstream of RAF-1 activation.

Enhanced phosphorylation of BIM_{EL} in BAG-1-expressing acini

BIM is a critical effector of luminal cell death in MCF-10A acini (Reginato et al., 2005). Its expression is regulated by ERK-mediated phosphorylation on serine 69 (S69), which subsequently targets it for proteasomal degradation (Ley et al., 2003; Luciano et al., 2003). BIM has a relatively short half-life (Meller et al., 2006), thus to enable optimal observation of BIM S69 phosphorylation, we blocked the activity of the proteasome using the proteasome inhibitor MG132 and examined expression of BIM at the earlier time points of days 5 and 6 of 3D culture. The cell cycle regulator, p21$^{WAF1/CIP1}$, was used as a positive control in these experiments, as it is known to be rapidly degraded by the proteasome (Blagosklonny et al., 1996). Figure 5b demonstrates that addition of MG132 resulted in an increase in BIM_{EL} S69 phosphorylation in both MCF-10A/BAG-1 and MCF-10A/VEC acini compared with vehicle-treated acini, however, this effect was significantly enhanced in BAG-1-expressing cells compared with vector controls.

MEK inhibition restores luminal apoptosis in BAG-1-expressing acini

To further establish the role of MEK–ERK activation in mediating BAG-1's prosurvival effects, we investigated the effects of the MEK inhibitor, U0126, on the BAG-1-induced phenotype in 3D culture. MCF-10A/BAG-1 and MCF-10A/VEC acini were treated with U0126 and whole-cell lysates were prepared for protein analysis at days 6 and 10 of 3D culture. Treatment of BAG-1-expressing acini with the vehicle (dimethyl sulfoxide) confirmed our earlier observations of an increase in ERK1/2 phosphorylation and decrease in BIM_{EL} expression compared with vector control acini at both
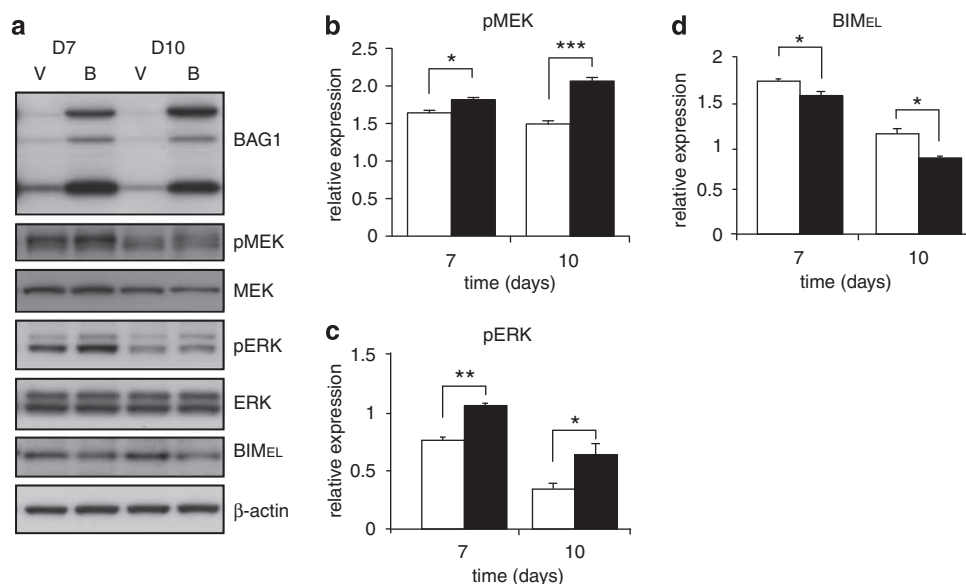

Figure 4 Bcl-2-associated anthanogene 1 (BAG-1) expression is associated with enhanced mitogen-activated kinase/ERK kinase–extracellular signal-regulated kinase (MEK–ERK) signaling. (**a**) Representative immunoblots of total and phosphorylated MEK1/2 and ERK1/2, and total BIM_{EL} expression in whole cell lysates from BAG-1-expressing (b) and vector control (V) acini at days 7 and 10 of three-dimensional (3D) culture. β-actin was used as an additional loading control. (**b**) Densitometry of MEK phosphorylation relative to total MEK in MCF-10A/BAG-1 (black bars) and MCF-10A/VEC (white bars) acini from at least three independent experiments. (**c**) Densitometry of ERK1/2 phosphorylation relative to total ERK in MCF-10A/BAG-1 (black bars) and MCF-10A/VEC (white bars) acini from at least three independent experiments. (**d**) Densitometry of BIM_{EL} expression normalized to β-actin in MCF-10A/BAG-1 (black bars) and MCF-10A/VEC (white bars) acini from at least three independent experiments. Error bars indicate s.e.m., *$P < 0.05$ for BAG-1-expressing acini versus vector controls.
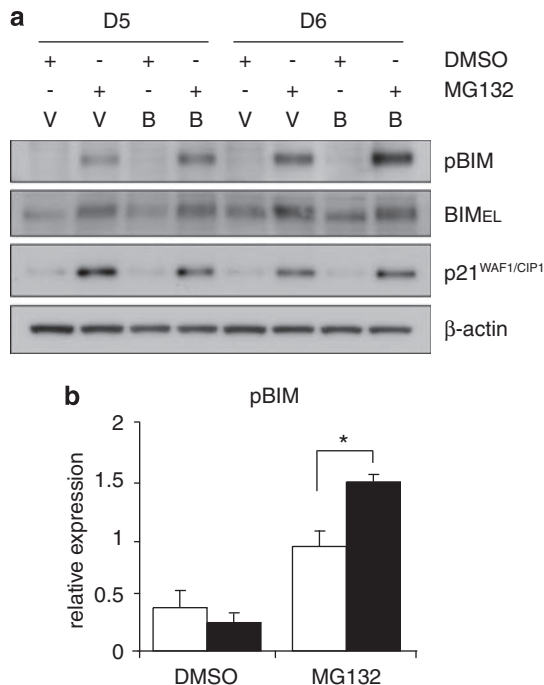
a

b

Figure 5 Inhibition of proteasomal degradation is associated with an increase in BIM serine 69 phosphorylation in Bcl-2-associated anthanogene 1 (BAG-1)-expressing acini. (**a**) Representative immunoblots of total BIM_{EL} and BIM_{EL} S69 phosphorylation in whole-cell lysates from BAG-1-expressing (b) and vector control (V) acini at days 5 and 6 of three-dimensional (3D) culture after a 5-h pre-treatment with the proteasome inhibitor, MG132, or vehicle (dimethyl sulfoxide; DMSO). Expression of p21$^{WAF1/CIP1}$ was used as a positive control for MG132 activity. β-actin was used as an additional loading control. (**b**) Densitometry of BIM_{EL} phosphorylation relative to total BIM_{EL} at day 6 in MCF-10A/BAG-1 (black bars) and MCF-10A/VEC (white bars) acini treated with MG132 or vehicle control from at least three independent experiments. Error bars indicate s.e.m., *$P < 0.05$ for BAG-1-expressing acini versus vector controls.

time points (Figures 6a and 4a). However, treatment with U0126 attenuated both these effects in BAG-1-expressing acini and levels of both phosphorylated ERK1/2 and BIM_{EL} were similar to levels observed in vector control cells (Figure 6a), confirming that active MEK–ERK signaling had been inhibited.

We then determined the effects of MEK inhibition on BAG-1-mediated survival using M30 expression at day 10 of 3D culture as a marker of acinar apoptosis. Data from vehicle-treated acini confirmed our earlier results that BAG-1 expression significantly attenuates apoptosis compared with vector control cells (Figures 6b and c, and 2a). However, treatment with U0126 ablated this survival effect and BAG-1-expressing acini displayed levels of apoptosis similar to those observed in vector control acini (Figure 6c). Thus, these data suggest that the BAG-1-induced survival phenotype in MCF-10A 3D acini is mediated via active MEK–ERK signaling leading to a decrease in BIM_{EL} expression through S69 phosphorylation and proteasomal degradation, and the subsequent loss of apoptotic signals in the central luminal space (Figure 7).

Discussion

The multi-functional, prosurvival protein, BAG-1 is commonly overexpressed in breast cancers (Sharp et al., 2004). However, although the dysregulation of apoptotic signaling cascades is a hallmark of malignancy (Hanahan and Weinberg, 2000), the role of BAG-1 in the development or progression of breast cancer remains ill defined. Here we have used the MCF-10A 3D model of mammary epithelial morphogenesis to address this and to further elucidate the mechanistic basis for BAG-1's actions in this context. This 3D model recapitulates many of the normal, morphogenic features of the mammary epithelium in vivo, including the formation of polarized spheroid structures or 'acini' containing a central, hollow lumen formed through a well-defined apoptotic program (Debnath et al., 2002; Mailleux et al., 2008), and has been used effectively to elucidate the role of oncogene-driven signaling pathways in the malignant process in a biologically relevant context (Debnath and Brugge, 2005).

The overexpression of BAG-1 in MCF-10A cells led to an attenuation of luminal apoptosis—characterized by an increased number of acini with filled lumens and a decrease in molecular markers of apoptosis such as M30 and activated caspase-3. This phenotype typifies those seen in most breast carcinomas and preinvasive lesions such as ductal carcinoma in situ, as well as some precancerous states such as atypical ductal hyperplasia (Harris et al., 1999), suggesting that disruption of the normal apoptotic program may have an important role in the initiation and progression of breast cancer. Studies aimed at elucidating the molecular mechanisms governing the formation and maintenance of the luminal space have demonstrated that it may be influenced both by Akt-mediated survival signals in the matrix-associated outer cells (Debnath et al., 2002) and active, BIM-mediated apoptotic signals in the centrally localized cells (Reginato et al., 2005; Mailleux et al., 2007). BIM is upregulated immediately before the initiation of apoptosis and is specifically inhibited by prosurvival oncoproteins through stimulation of MEK–ERK signaling (Reginato et al., 2005). However, overexpression of anti-apoptotic regulators, such as BCL-2 and BCL-XL, only delays but does not completely ablate luminal apoptosis in 3D acini (Debnath et al., 2002). The latter requires an enhancement of both proliferative and anti-apoptotic cues such as those provided by the epidermal growth factor receptor, ERBB2/HER2 (Muthuswamy et al., 2001), or through co-expression of proliferation and survival proteins (Debnath et al., 2002).

Thus, these data demonstrating that BAG-1 expression maintains luminal filling up to 20 days in 3D culture suggest that it may elicit this phenotype by influencing pathways controlling both cellular survival and proliferation—a concept further supported by our observations of enhanced RAF-1 activation in BAG-1-expressing acini. Signaling cascades downstream of RAF-1 are known to influence both mitogenic and anti-apoptotic pathways, for example, through the regulation of the proliferative genes FOS and MYC
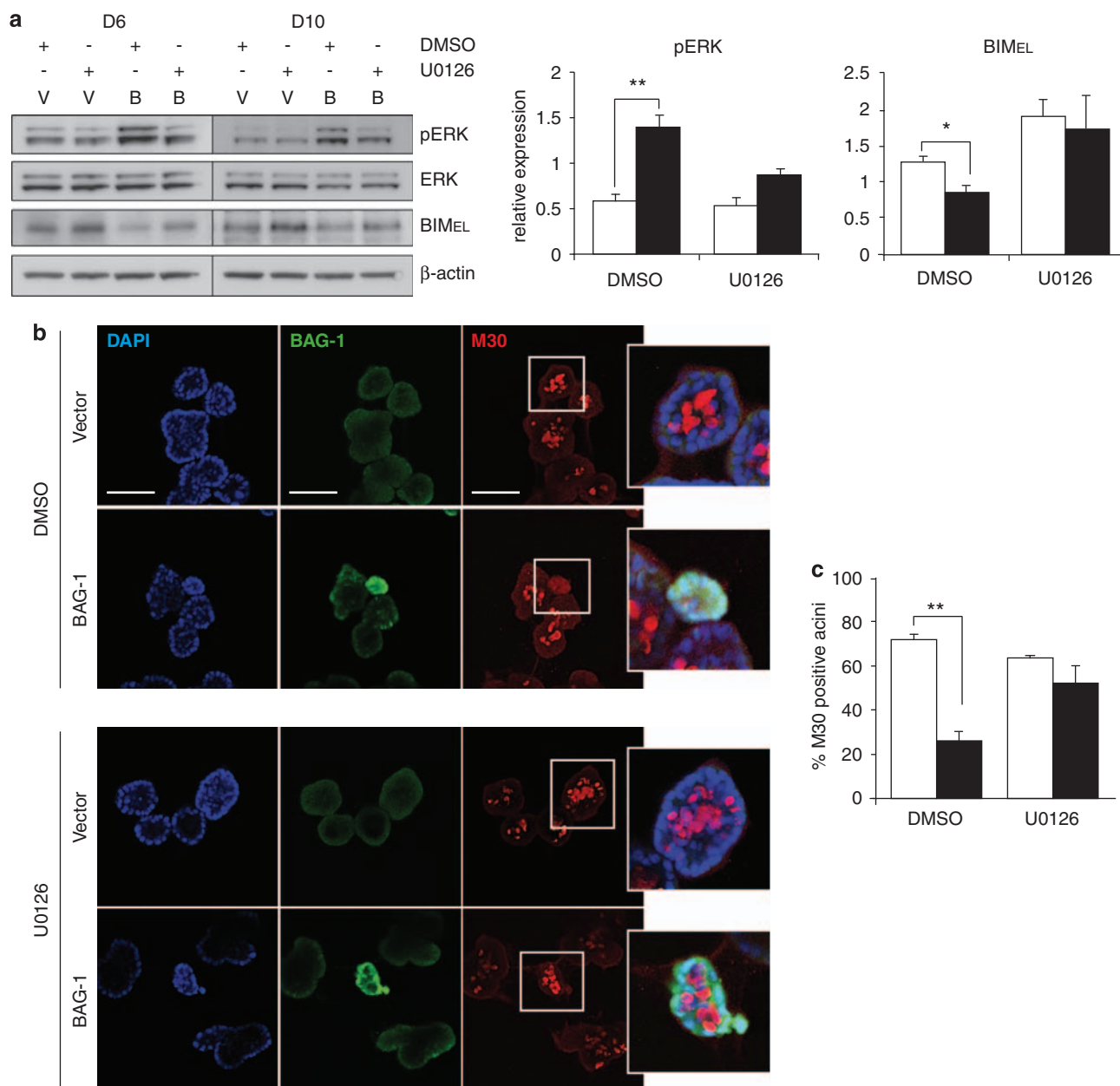
Figure 6 Inhibition of mitogen-activated kinase/ERK kinase–extracellular signal-regulated kinase (MEK–ERK) signaling reverses Bcl-2-associated anthanogene 1 (BAG-1)-mediated attenuation of luminal apoptosis in three-dimensional (3D) acini. (**a**) Representative immunoblots of total and phosphorylated ERK1/2 and BIM_{EL} expression in whole-cell lysates from BAG-1-expressing (b) and vector control (*V*) acini at days 6 and 10 of 3D culture after treatment with U0126 or vehicle control (dimethyl sulfoxide; DMSO). β-actin was used as an additional loading control. Graphs show densitometry of phosphorylated ERK1/2 and BIM_{EL} expression at day 10 normalized to total ERK or β-actin in MCF-10A/BAG-1 (black bars) and MCF-10A/VEC (white bars) acini from at least two independent experiments. Error bars indicate s.e.m., *$P < 0.05$; **$P < 0.02$ for BAG-1-expressing acini versus vector controls. (**b**) Representative equatorial confocal cross-sections showing M30 (apoptosis), BAG-1 and 4′,6-diamidino-2-phenylindole (DAPI) staining in BAG-1-expressing and vector control acini at day 10 of three-dimensional (3D) culture after treatment with the mitogen-activated kinase/ extracellular signal-regulated kinase kinase (MEK) inhibitor, U0126, or vehicle control (dimethyl sulfoxide, DMSO). Overlays of selected sections are shown in white boxes. Scale bars = 100 µm. (**c**) Graph represents quantification of positive M30 staining (containing ⩾4 M30-positive cells) in MCF-10A/BAG-1 (black bars) and MCF-10A/VEC (white bars) acini at day 10 from at least three independent experiments. Error bars indicate s.e.m., **$P < 0.005$ for BAG-1-expressing acini versus vector controls.

and the apoptotic regulators BAD, BIM and BCL-2 (Kolch, 2000), and although this study predominantly focused on apoptotic endpoints, it is plausible that BAG-1's interactions with RAF-1 are influencing both these processes in 3D acini. In addition, BAG-1 directly interacts with the cell-cycle regulatory protein, Retinoblastoma (Arhel *et al.*, 2003) that itself is a RAF-1 substrate (Wang *et al.*, 1998) and increases the proliferation rate of neuronal precursor cells (Elliott and Ginzburg, 2009).

Attenuation of the BAG-1-associated survival phenotype by the MEK inhibitor, U0126, confirms that the RAF-1 signaling cascade is a major pathway through which BAG-1 mediates its effects in this model. Although this is in contrast to BAG-1's role in protecting against heat shock-induced apoptosis, in which its survival effects are dependent on HSP70/HSC70 binding and not on interaction with RAF-1 (Townsend et al., 2003a), it is perhaps not surprising given the pleiotropic nature of BAG-1's actions and those of its interacting partners, and it emphasizes the importance of delineating the functional effects of BAG-1 in a context-specific manner. This is further reflected by the fact that known regulators of BAG-1/RAF-1 survival signaling in other cell types, such as BCL-2 or BAD, were not altered in BAG-1-expressing MCF-10A cells (data not shown), suggesting that BIM-mediated effects may predominate in this model. Given the strong phenotypic correlations between the MCF-10A 3-D model and mammary morphogenesis in vivo (Debnath and Brugge, 2005), these data also suggest that the BAG-1–RAF-1 interaction may be of importance in the early phases of breast cancer development through a disruption in the normal cellular architecture of the mammary gland. Indeed, the elevated levels of BAG-1 expression observed in early breast lesions and preinvasive breast cancers such as ductal carcinoma in situ (Brimmell et al., 1999) would further support a role for BAG-1 in the development of breast carcinogenesis. Interestingly, several studies have also shown increased MAP kinase activity in breast cancers compared with benign breast tissue (Sivaraman et al., 1997; Salh et al., 1999; Mueller et al., 2000), with evidence that in at least some cases, this is independent of Ras mutations or elevated growth factor receptor expression (Mueller et al., 2000). We would postulate on the basis of our data that BAG-1 overexpression may provide an alternative mechanism by which enhanced MAP kinase signaling is initiated in breast cancers. Thus, further studies examining the correlation between BAG-1 expression and RAF-1 or MAP kinase activity in breast cancer tissue would be of interest.

Although these experiments were primarily focused on the role of BAG-1 in the development of the malignant process in the breast, it is nonetheless of interest to speculate how they may relate to the association between high BAG-1 expression and improved outcome for breast cancer patients observed by us and others (Turner et al., 2001; Cutress et al., 2003; Millar et al., 2008; Nadler et al., 2008). One possible explanation for this apparent dichotomy lies in the inherent heterogeneity in BAG-1's actions, such that its pro-survival effects may have an important role during tumor initiation, but lead to the formation of a less aggressive or more therapeutically responsive cancer, for example, through its known effects on nuclear hormone receptor function. However, interpretation of immunohistochemical studies of BAG-1 expression in breast cancer tissue are also confounded by differences in the intracellular localization and hence, possibly the BAG-1 isoform being detected, await analyses using isoform-specific antibodies to be fully resolved. It would also be of further interest to determine which of the three major isoforms of BAG-1 are mediating the effects observed in our 3D model.

In summary, we have demonstrated that expression of BAG-1 in immortalized mammary epithelial cells grown in 3D cultures phenocopies changes observed in preinvasive breast cancers such as ductal carcinoma in situ, namely a decrease in apoptosis and a filling of the central luminal space. As illustrated in Figure 7, these effects are mediated through the activation of the serine/threonine kinase RAF-1, with supporting evidence of a direct interaction with BAG-1. This leads to the subsequent activation of a downstream signaling cascade through the phosphorylation of MEK and ERK1/2. The latter phosphorylates BIM_{EL} on serine 69 targeting it for proteasomal degradation, resulting in the loss of normal apoptotic signals in the lumen and a filled luminal space. Thus, these studies not only provide important new insight into the factors governing breast cancer development, but also suggest that targeting BAG-1 or BAG-1–RAF-1 interactions may provide an effective new strategy for therapeutic intervention.
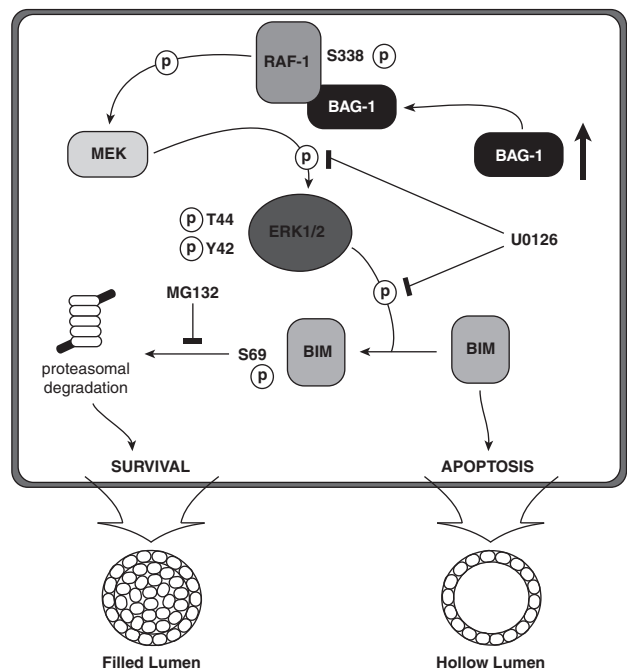

Figure 7 A schematic representation of the putative intracellular signaling pathways mediating Bcl-2-associated anthanogene 1 (BAG-1) effects on the apoptotic program during MCF-10A morphogenesis in three-dimensional (3D) culture. Increased expression of BAG-1 results in an activation of RAF-1 through the phosphorylation of serine 338 (S338). This initiates a downstream signaling cascade resulting in enhanced phosphorylation of BIM_{EL} on serine 69 (S69) by activated ERK1/2. Phosphorylated BIM_{EL} is rapidly targeted for proteasomal degradation leading to a decrease in its expression levels and a loss of normal pro-apoptotic signaling in the luminal space. The mitogen-activated kinase/extracellular signal-regulated kinase kinase (MEK) inhibitor, U0126, blocks the activity of MEK and extracellular signal-regulated kinase 1/2 (ERK1/2) resulting in a restoration of BIM_{EL} expression and activity, and the formation of hollow acinar structures through activation of apoptosis in the central luminal space.

Materials and methods

Human breast cell lines

The panel of normal, immortalized and breast cancer cell lines (Figure 1) were all obtained from ATCC (American Type Culture Collection, Manassas, VA, USA) except HMEC 219-4 (Clonetics, Lonza Australia, Mt Waverley, VIC, Australia), HMEC 184, HMEC 184-A1 and HMEC 184-B5 (a kind gift from Dr Martha Stampfer, Berkeley, CA, USA). Characteristics of these cell lines have been described previously (Sutherland et al., 1999).

Retroviral vectors

A complementary DNA insert encoding human BAG-1 (cat no. SC107955; OriGene Technologies, Rockville, MD, USA) was subcloned into EcoR1 and Not1 sites in the gateway vector pENTR2B. LR clonase recombination reaction was then used to transfer the complementary DNA insert encoding human BAG-1 into the retroviral vector pQCXIP (Invitrogen, Carlsbad, CA, USA).

Cell culture and retroviral infection of MCF-10A cells

MCF-10A and MCF-10A/EcoR cells (MCF-10A cells expressing the ecotropic retroviral receptor; a kind gift from Drs Danielle Lynch and Joan Brugge, Department of Cell Biology, Harvard Medical School, Boston, MA, USA), were routinely maintained in monolayer culture in Dulbecco's modified Eagles's medium/nutrient mixture F-12 (Invitrogen) supplemented with 5% (v/v) horse serum (Invitrogen), 100 ng/ml cholera toxin (Sigma, St. Louis, MO, USA), 20 ng/ml human recombinant epidermal growth factor (R&D Systems, Minneapolis, MN, USA), 0.5 µg/ml hydrocortisone (Sigma), 50 U/ml penicillin G (Invitrogen), and 50 µg/ml streptomycin sulfate (Invitrogen). For co-immunoprecipitation studies, cells were serum-starved in 0.4% (v/v) horse serum for 18 h before addition of 100 ng/ml epidermal growth factor for 5 mins. For 3D cultures, MCF-10A cells were grown as previously described (Debnath et al., 2003).

Retrovirus was constructed essentially as previously described (Brummer et al., 2006). Briefly, the ecotropic packaging cell line PlatE was transfected with the BAG-1 construct using Fugene (Roche, Nutley, NJ, USA). Retrovirus was collected 48 h post-transfection, diluted with medium and then added to subconfluent MCF-10A/EcoR cells. Infected cells were selected for 1 week in puromycin (2 µg/ml; Life Technologies, Carlsbad, CA, USA) to yield stable retroviral pools.

The 3D cultures were generated by plating single-cell suspensions into chamber slides (BD Falcon, Franklin Lakes, NJ, USA) that had been previously coated with a thin-layered growth factor-reduced Matrigel (BD Biosciences). The day of plating was taken as day 0 and the medium was replaced every 4 days. Inhibitors were added as follows: U0126 (0.5 µM; Sigma) at the specified dose on day 5 of 3D culture, and the medium was replaced every 2 days after; MG132 (50 µM; R&D Systems) 5 h before collection.

Analysis of 3D matrigel cultures by confocal microscopy

For confocal microscopy, acini were fixed and stained using the indicated antibodies as described earlier (Debnath et al., 2003). Acini were then stained using the appropriate Cy3- or Cy2-labeled secondary antibodies (Jackson ImmunoResearch Laboratories, West Grove, PA, USA) and 4′,6-diamidino-2-phenylindole as a DNA counterstain. Antibody specificity was confirmed by using the following controls: primary antibody with no secondary labeled antibody and secondary labeled antibody with no primary antibody. Confocal microscopy was performed using either Leica DMRBE (SP1) or Leica DMIRE2 (SP2 AOBS) confocal microscope (Leica Microsystems, North Ryde, NSW, Australia). For colocalization studies, analysis was performed by compiling multiple high-resolution z stacks of x and y plane confocal scans using Leica confocal software. M30 was quantified by scoring at least 100 structures using a fluorescence microscope. Acini that contained more than four M30-positive cells were scored as positive.

Acini were collected essentially as previously described (Caldon et al., 2008). Briefly, Matrigel was dissolved using cell recovery solution (BD Biosciences) following the manufacturer's instructions. Chamber slides were then washed in phosphate buffered saline and the acini were collected by centrifugation and then lysed using ice-cold lysis buffer (50 mmol/l HEPES (pH 7.4), 0.1% (w/v) SDS, 1% (v/v) Triton X-100, 0.5% (w/v) sodium deoxycholate, 5 mmol/l EDTA, 10 µg/ml aprotinin, 10 µg/ml leupeptin, 1 mmol/l phenylmethylsulfonyl fluoride, 50 mmol/l sodium fluoride, and 1 mmol/l sodium orthovanadate).

Real-time quantitative PCR

Total RNA was isolated using the RNAeasy kit (Qiagen, Doncaster, VIC, Australia) and was reverse-transcribed using the Reverse Transcription System (Promega, Alexandria, NSW, Australia) according to manufacturer's instructions. Real-time PCR was performed with an ABI Prism 7900HT Sequence Detection System (Applied Biosystems, Foster City, CA, USA) using inventoried (pre-made) Taq-Man probes for BAG-1 (Applied Biosystems). Data analyses were performed using the ΔDC_t method with RPLPO (Applied Biosystems) as an internal loading control. Fold changes in gene expression were calculated relative to untreated controls.

Western blot analysis

Whole cell protein lysates (10–30 µg) were separated using NuPAGE polyacrylamide gels (Invitrogen) and transferred to polyvinylidine difluoride membranes (Bio-Rad Laboratories, Hercules, CA, USA) using standard methods.

Antibodies

Antibodies against phospho-Ser[69] BIM, phospho-Ser[338] RAF-1, phosphorylated and total p42/44 ERK, MEK1/2, and cleaved caspase-3 were purchased from Cell Signaling Technology (Danvers, MA, USA). Anti-BIM antibody was purchased from Calbiochem (San Diego, CA, USA). Anti-BAG-1 antibodies (clone 3.10G3E2, immunoblotting and Y166, immunofluorescence) were purchased from Chemicon International (Billerica, MA, USA) and Abcam (Cambridge, MA, USA), respectively. Anti-RAF-1 (C12) antibody was purchased from Santa Cruz Biotechnology (Santa Cruz, CA, USA). Anti-M30 CytoDEATH antibody was purchased from Alexis Biochemicals (San Diego, CA, USA); anti-β-actin (Clone AC-15) antibody was purchased from Sigma; anti-p21[WAF1/CIP1] (C24420) and anti-β-catenin antibodies were purchased from BD Biosciences.

Immunoprecipitation

MCF-10A/VEC and MCF-10A/BAG-1 cells were grown in monolayer, collected and immunoprecipitated using 2 µg of either anti-RAF-1 (C-12) antibody or negative control (normal rabbit IgG; Santa Cruz Biotechnology) essentially as previously described (Townsend et al., 2003a).

Densitometry and statistical analysis
Densitometry was performed using ImageJ 1.37v. software (National Institutes of Health, Bethesda, MD, USA) and statistical analyses were performed using a two-sided Student's *t*-test in GraphPad Prism 5 (GraphPad Software, La Jolla, CA, USA) following Log10 transformation where appropriate (Figure 1). A *P*-value of <0.05 was considered to be statistically significant.

Abbreviations

BAG-1, Bcl-2-associated anthanogene; ERK, extracellular signal regulated kinase; MEK, mitogen-activated kinase/ERK kinase; ER, estrogen receptor; DCIS, ductal carcinoma *in situ*; 3D, three-dimensional; DAPI, 4′,6-diamidino-2-phenylindole.

Conflict of Interest

The authors declare no conflict of interest.

References

Arhel NJ, Packham G, Townsend PA, Collard TJ, H-Zadeh AM, Sharp A *et al.* (2003). The retinoblastoma protein interacts with Bag-1 in human colonic adenoma and carcinoma derived cell lines. *Int J Cancer* **106**: 364–371.

Avruch J, Zhang XF, Kyriakis JM. (1994). Raf meets Ras: completing the framework of a signal transduction pathway. *Trends Biochem Sci* **19**: 279–283.

Blagosklonny MV, Wu GS, Omura S, el-Deiry WS. (1996). Proteasome-dependent regulation of p21WAF1/CIP1 expression. *Biochem Biophys Res Commun* **227**: 564–569.

Brimmell M, Burns JS, Munson P, McDonald L, O′Hare MJ, Lakhani SR *et al.* (1999). High level expression of differentially localized BAG-1 isoforms in some oestrogen receptor-positive human breast cancers. *Brit J Cancer* **81**: 1042–1051.

Brummer T, Schramek D, Hayes VM, Bennett HL, Caldon CE, Musgrove EA *et al.* (2006). Increased proliferation and altered growth factor dependence of human mammary epithelial cells overexpressing the Gab2 docking protein. *J Biol Chem* **281**: 626–637.

Caldon CE, Swarbrick A, Lee CS, Sutherland RL, Musgrove EA. (2008). The helix-loop-helix protein Id1 requires cyclin D1 to promote the proliferation of mammary epithelial cell acini. *Cancer Res* **68**: 3026–3036.

Cutress RI, Townsend PA, Sharp A, Maison A, Wood L, Lee RS *et al.* (2003). The nuclear BAG-1 isoform, BAG-1L, enhances oestrogen-dependent transcription. *Oncogene* **22**: 4973–4982.

Debnath J, Brugge J. (2005). Modelling glandular epithelial cancers in three-dimensional cultures. *Nature Reviews Cancer* **5**: 675–688.

Debnath J, Mills KR, Collins NL, Reginato MJ, Muthuswamy SK, Brugge J. (2002). The role of apoptosis in creating and maintaining luminal space within normal and oncogene-expressing mammary acini. *Cell* **111**: 29–40.

Debnath J, Muthuswamy SK, Brugge J. (2003). Morphogenesis and oncogenesis of MCF-10A mammary epithelial acini grown in three-dimensional basement membrane cultures. *Methods* **30**: 256–268.

Elliott E, Ginzburg I. (2009). BAG-1 is preferentially expressed in neuronal precursor cells of the adult mouse brain and regulates their proliferation *in vitro*. *FEBS Lett* **583**: 229–234.

Froesch BA, Takayama S, Reed JC. (1998). BAG-1 L protein enhances androgen receptor function. *J Biol Chem* **273**: 11660–11666.

Hanahan D, Weinberg RA. (2000). The hallmarks of cancer. *Cell* **200**: 57–70.

Harris JR, Lippman ME, Morrow M, Osborne CK. (1999). *Diseases of the breast*. Lippincott Williams and Wilkins: Philadelphia.

Höhfeld J. (1998). Regulation of the heat shock conjugate Hsc70 in the mammalian cell: the characterization of the anti-apoptotic protein BAG-1 provides novel insights. *Biol Chem* **379**: 269–274.

Kolch W. (2000). Meaningful relationships: the regulation of the Ras/Raf/MEK/ERK pathway by protein interactions. *Biochem J* **351**: 289–305.

Kudoh M, Knee DA, Takayama S, Reed JC. (2002). Bag1 proteins regulate growth and survival of ZR-75-1 human breast cancer cells. *Cancer Res* **62**: 1904–1909.

Ley R, Balmanno K, Hadfield K, Weston C, Cook SJ. (2003). Activation of the ERK1/2 signaling pathway promotes phosphorylation and proteasome-dependent degradation of the BH3-only protein, Bim. *J Biol Chem* **278**: 18811–18816.

Luciano F, Jacquel A, Colosetti P, Herrant M, Cagnol S, Pages G *et al.* (2003). Phosphorylation of Bim-EL by Erk1/2 on serine 69 promotes its degradation via the proteasome pathway and regulates its proapoptotic function. *Oncogene* **22**: 6785–6793.

Mailleux AA, Overholtzer M, Brugge JS. (2008). Lumen formation during mammary epithelial morphogenesis: insights from *in vitro* and *in vivo* models. *Cell cycle* **7**: 57–62.

Mailleux AA, Overholtzer M, Schmelzle T, Bouillet P, Strasser A, Brugge JS. (2007). BIM regulates apoptosis during mammary ductal morphogenesis, and its absence reveals alternative cell death mechanisms. *Dev Cell* **12**: 221–234.

Meller R, Cameron JA, Torrey DJ, Clayton CE, Ordonez AN, Henshall DC *et al.* (2006). Rapid degradation of Bim by the ubiquitin–proteasome pathway mediates short-term ischemic tolerance in cultured neurons. *J Biol Chem* **281**: 7429–7436.

Millar EKA, Anderson LR, McNeil CM, O′Toole SA, Pinese M, Crea P *et al.* (2008). BAG-1 predicts patient outcome and tamoxifen responsiveness in ER-positive invasive ductal carcinoma of the breast. *Br J Cancer* **100**: 123–133.

Mueller H, Flury N, Eppenberger-Castori S, Kueng W, David F, Eppenberger U. (2000). Potential prognostic value of mitogen-activated protein kinase activity for disease-free survival of primary breast cancer patients. *Int J Cancer* **89**: 384–388.

Muthuswamy SK, Li D, Lelievre S, Bissell MJ, Brugge JS. (2001). ErbB2, but not ErbB1, reinitiates proliferation and induces luminal repopulation in epithelial acini. *Nat Cell Biol* **3**: 785–792.

Nadler Y, Camp RL, Giltnane JM, Moeder C, Rimm DL, Kluger HM *et al.* (2008). Expression patterns and prognostic value of Bag-1 and Bcl-2 in breast cancer. *Breast Cancer Res* **10**: R35.

Packham G, Brimmell M, Cleveland JL. (1997). Mammalian cells express two differently localized Bag-1 isoforms generated by alternative translation initiation. *Biochem J* **328**: 807–813.

Reginato MJ, Mills KR, Becker EBE, Lynch DK, Bonni A, Muthuswamy SK *et al.* (2005). Bim regulation of lumen formation in cultured mammary epithelial acini is targeted by oncogenes. *Mol Cell Biol* **25**: 4591–4601.

538

Salh B, Marotta A, Matthewson C, Ahluwalia M, Flint J, Owen D *et al.* (1999). Investigation of the Mek–MAP kinase–Rsk pathway in human breast cancer. *Anticancer Res* **19**: 731–740.

Sharp A, Crabb SJ, Townsend PA, Cutress RI, Brimmell M, Wang XH *et al.* (2004). BAG-1 in carcinogenesis. *Expert Rev Mol Med* **6**: 1–15.

Sivaraman VS, Wang H, Nuovo GJ, Malbon CC. (1997). Hyper-expression of mitogen-activated protein kinase in human breast cancer. *J Clin Invest* **99**: 1478–1483.

Song J, Takeda M, Morimoto RI. (2001). Bag1-Hsp70 mediates a physiological stress signalling pathway that regulates Raf-1/ERK and cell growth. *Nat Cell Biol* **3**: 276–282.

Sutherland RL, Watts CK, Lee CSL, Musgrove EA. (1999). Breast Cancer. In: Masters JRW and Palsson B (eds). *Human Cell Culture*. Kluwer: Dordrecht, pp 79–106.

Takayama S, Bimston DN, Matsuzawa S, Freeman BC, Aime-Sempe C, Xie Z *et al.* (1997). BAG-1 modulates the chaperone activity of Hsp70/Hsc70. *EMBO J* **16**: 4887–4896.

Takayama S, Krajewski S, Krajewska M, Kitada S, Zapata JM, Kochel K *et al.* (1998). Expression and location of Hsp70/Hsc-binding anti-apoptotic protein BAG-1 and its variants in normal tissues and tumor cell lines. *Cancer Res* **58**: 3116–3131.

Takayama S, Sato T, Krajewski S, Kochel K, Irie S, Millan JA *et al.* (1995). Cloning and functional analysis of BAG-1: a novel Bcl-2-binding protein with anti-cell death activity. *Cell* **80**: 279–284.

Townsend PA, Cutress RI, Sharp A, Brimmell M, Packham G. (2003a). BAG-1 prevents stress-induced long-term growth inhibition in breast cancer cells via a chaperone-dependent pathway. *Cancer Res* **63**: 4150–4157.

Townsend PA, Cutress RI, Sharp A, Brimmell M, Packham G. (2003b). BAG-1: a multifunctional regulator of cell growth and survival. *Biochim Biophys Acta* **1603**: 83–98.

Townsend PA, Dublin E, Hart IR, Kao R-H, Hanby AM, Cutress RI *et al.* (2002). BAG-1 expression in human breast cancer: inter-relationship between BAG-1 RNA, protein, HSC70 expression and clinico-pathological data. *J Pathol* **197**: 51–59.

Turner BC, Krajewski S, Krajewska M, Takayama S, Gumbs AA, Carter D *et al.* (2001). BAG-1: a novel biomarker predicting long-term survival in early stage-breast cancer. *J Clin Oncol* **19**: 992–1000.

Wang H-G, Takayama S, Rapp UR, Reed JC. (1996). Bcl-2 interacting protein, BAG-1, binds to and activates the kinase Raf-1. *Proc Natl Acad Sci USA* **93**: 7063–7068.

Wang S, Ghosh RN, Chellappan SP. (1998). Raf-1 physically interacts with Rb and regulates its function: a link between mitogenic signaling and cell cycle regulation. *Mol Cell Biol* **18**: 7487–7498.

Wang X-H, O'Connor D, Brimmell M, Packham G. (2009). The BAG-1 cochaperone is a negative regulator of p73-dependent transcription. *Brit J Cancer* **100**: 1347–1357.

Yang XL, Hao Y, Ding Z, Pater A, Tang S-C. (1999). Differential expression of antiapoptotic gene BAG-1 in human breast normal and cancer cell lines and tissues. *Clin Cancer Res* **5**: 1816–1822.

Zeiner M, Gehring U. (1995). A protein that interacts with members of the nuclear hormone receptor family: identification and cDNA cloning. *Proc Natl Acad Sci USA* **92**: 11465–11469.